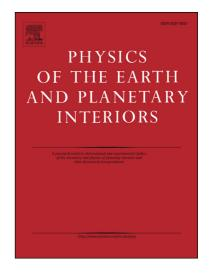
# Accepted Manuscript

ISC-GEM: Global Instrumental Earthquake Catalogue (1900-2009), II. Location and Seismicity Patterns

I. Bondár, E. Robert Engdahl, A. Villaseñor, James Harris, D. Storchak

PII:	\$0031-9201(14)00147-2
DOI:	http://dx.doi.org/10.1016/j.pepi.2014.06.002
Reference:	PEPI 5750
To appear in:	Physics of the Earth and Planetary Interiors
Received Date:	2 August 2013
Revised Date:	18 February 2014
Accepted Date:	2 June 2014



Please cite this article as: Bondár, I., Robert Engdahl, E., Villaseñor, A., Harris, J., Storchak, D., ISC-GEM: Global Instrumental Earthquake Catalogue (1900-2009), II. Location and Seismicity Patterns, *Physics of the Earth and Planetary Interiors* (2014), doi: http://dx.doi.org/10.1016/j.pepi.2014.06.002

This is a PDF file of an unedited manuscript that has been accepted for publication. As a service to our customers we are providing this early version of the manuscript. The manuscript will undergo copyediting, typesetting, and review of the resulting proof before it is published in its final form. Please note that during the production process errors may be discovered which could affect the content, and all legal disclaimers that apply to the journal pertain.

# ISC-GEM: Global Instrumental Earthquake Catalogue

#### (1900-2009), II. Location and Seismicity Patterns

I. Bondár<sup>1</sup>, E. Robert Engdahl<sup>2</sup>, A. Villaseñor<sup>3</sup>, James Harris<sup>1</sup>, and D. Storchak<sup>1</sup>

SCR

1) International Seismological Centre, UK.

2) University of Colorado at Boulder, USA.

3) Institute of Earth Sciences Jaume Almera, Spain.

Corresponding Author: István Bondár, istvan@isc.ac.uk <

#### Abstract

We present the final results of a two-year project sponsored by the Global Earthquake Model (GEM) Foundation. The ISC-GEM global catalogue consists of some 19 thousand instrumentally recorded, moderate to large earthquakes, spanning 110 years of seismicity. We relocated all events in the catalogue using a two-tier approach. The EHB location methodology (Engdahl et al., 1998) was applied first to obtain improved hypocentres with special focus on the depth determination. The locations were further refined in the next step by fixing the depths to those from the EHB analysis and applying the new International Seismological Centre (ISC) location algorithm (Bondár and Storchak, 2011) that reduces location bias by accounting for correlated travel-time prediction error structure. To facilitate the relocation effort, some one million seismic P and S wave arrival-time data were added to the ISC database for the period between 1904 and 1970, either from original station bulletins in the ISC archive or by digitizing the scanned images of the International

Seismological Summary (ISS) bulletin (Villaseñor and Engdahl, 2005; 2007). Although no substantial amount of new phase data were acquired for the modern period (1964-2009), the number of phases used in the location has still increased by three millions, owing to fact that both the EHB and ISC locators use most wellrecorded *ak135* (Kennett et al., 1995) phases in the location.

We show that the relocation effort yielded substantially improved locations, especially in the first half of the 20<sup>th</sup> century; we demonstrate significant improvements in focal depth estimates in subduction zones and other seismically active regions; and we show that the ISC-GEM catalogue provides an improved view of 110 years of global seismicity of the Earth. The ISC-GEM Global Instrumental Earthquake Catalogue represents the final product of one of the ten global components in the GEM program, and is available to researchers at the ISC (www.isc.ac.uk) website.

#### Introduction

We describe the two-year effort to produce a global instrumental catalogue for the Global Earthquake Model project (GEM, <u>www.globalquakemodel.org</u>). The GEM Foundation is a public-private partnership that drives a collaborative effort aimed at developing and deploying tools and resources for earthquake risk assessment worldwide. The ISC-GEM Global Instrumental Catalogue represents one of the global components of the GEM project and consists of 18,809 large and moderate earthquakes that have occurred during the 110-year period between 1900 and 2009.

In the past, several earthquake catalogues were produced with the aim of documenting earthquakes that have occurred during the era of instrumental seismology (e.g. Abe,

1981, 1984; Abe and Noguchi, 1983a, 1983b; Gutenberg and Richter, 1954; Båth and Duda, 1979; Utsu, 1979, 1982a, 1982b; and Pacheco and Sykes, 1992). The most recent comprehensive catalogue is the Centennial Catalogue (Engdahl and Villaseñor, 2002) that covers the period 1900-2008. However, even the Centennial Catalogue is inhomogenous in the sense that not all earthquakes were relocated and the earthquake magnitudes were not recalculated.

The motivation of this project was to produce a comprehensive catalogue of large and moderate earthquakes for the entire instrumental period where each earthquake is relocated with the same location procedures; body and surface wave magnitudes are recalculated using the original amplitude-period measurements; and finally, each earthquake is characterized by either a direct measurement of  $M_W$ , or an  $M_W$  proxy estimate based on non-linear regressions between  $M_S-M_W$  and  $m_b-M_W$ . Such a global instrumental catalogue produced by uniform procedures would serve as input for the global seismic hazard and risk components of the GEM project.

To achieve this goal, we manually entered a substantial number of phase arrival times, and amplitude-period data from the original station bulletins in the ISC archive. We also added phase arrival time data from digitally available sources that were not already in the ISC database. The general overview of the project is given in Storchak et al. (2014); the data collection effort is described in detail in Di Giacomo et al. (2014a); and the procedures for computing body and surface wave magnitudes, as well as the derivation of the nonlinear regression relations are discussed in Di Giacomo et al. (2014b). In this paper we focus on the ISC-GEM location procedures and results.

#### Data

Due to limitations in resources, time and data availability, we introduced time-varying magnitude cut-offs for the earthquakes to be included in the ISC-GEM catalogue. For the earliest instrumental period (1900-1917) the decisive factor of including events was data availability due to the sparse distribution of seismological stations in the global network. In the early instrumental period (1918-1959) many more seismological stations were deployed but, except for a fraction of digitally available data, most of the phase arrival time data still had to be entered manually. Thus, for this period the available resources and time represented major limitations. For the modern instrumental period (1960-2009) the vast majority of phase arrival time data was already in the ISC database. With these limiting factors in mind, we set the magnitude cut-offs below for the ISC-GEM event selection.

- 1900-1917: M<sub>S</sub> ≥ 7.5 worldwide, as well as a selection of shallow events (M<sub>S</sub> ≥ 6.5) in stable continental areas;
- 1918-1959:  $M_S \ge 6.25$ ;
- 1960-2009:  $M_S \ge 5.5$ .

The ISC came into existence in 1964, and all data that have ever been published in the ISC bulletin are stored in the ISC database. Between 1918 and 1964 the major data source is the ISS (the predecessor of ISC) bulletin. Villaseñor and Engdahl (2007) have already relocated earthquakes in the ISS bulletin during the period 1960-1963 and thus the phase data were available in the ISC database. The ISC and the ISS bulletins in the ISC database provided 11 million and 330,000 phase picks for the

ISC-GEM events, respectively. For the period 1900-1959, the ISC database contained no phase arrival time data at all.

To fill in the gap we added some 230,000 phase picks from the Shannon tapes - the partially digitized ISS bulletin data between 1918 and 1942 owing to the initiative of the first two directors of the ISC, Pat Willmore and Edouard Arnold. The Japan Meteorological Agency (JMA) made its early instrumental bulletin between 1923-1970 available to us and it yielded some 270,000 picks from 230 stations for events in the ISC-GEM catalogue. The entire ISS bulletin (1918-1963) has been scanned by Storia Geofisica Ambiente, Bologna, Italy in the frame of the Euroseismos project (<u>www.storing.ingv.it/es\_web</u>). For events for which phase picks were not already digitally available we used optical character recognition software to digitize the scanned ISS bulletin pages. This effort resulted in some 400,000 phase picks between 1918 and 1959.

The rest of the phase arrival data were added manually. The British Association for the Advancement of Science (BAAS, predecessor of the ISS) bulletins yielded 3,800 picks for the period 1913-1917; the Gutenberg notepads (1904-1917) and the International Seismological Association (ISA, 1904-1907) provided 1,900 phase picks. Further 270,000 phase picks from 90 stations between 1904 and 1970 were manually entered into the database directly from original stations bulletins collected in the ISC archives.

For the period 1900-1903 no sufficient volume of reliable parametric station data were found to allow standard relocation and magnitude estimation. Hence the hypocentre parameters of earthquakes during this period were adopted from Abe and Noguchi (1983a; 1983b).

Erroneous station coordinates may adversely affect earthquake location results. To avoid this pitfall, we conducted a rigorous joint review of station parameters (coordinates and elevations) using ISC, U.S. Geological Survey, National Earthquake Information Center (NEIC) and U.S. Department of Energy, Lawrence Livermore National Laboratory (LLNL) source materials, largely for those stations that have reported to the ISC from 1964 to the present. Most inconsistencies have been resolved and new revised lists of station parameters and alternate station codes have been created for EHB and ISC implementation. A new feature of the station list is the addition of time periods over which the station parameters are valid, including many entries of stations with identical station codes but with different operational time periods.

# **Earthquake Relocation**

In order to obtain improved locations for the ISC-GEM catalogue over the period 1904-2009, we follow a two-tier procedure using the EHB (Engdahl et al., 1998) and the ISC (Bondár and McLaughlin, 2009a; Bondár and Storchak, 2011) location algorithms. Both the EHB and ISC location algorithms use most well-recorded reported phases in line with the IASPEI standard (Storchak et al., 2003 and 2011) with a valid *ak135* (Kennett et al., 1995) 1D travel-time prediction in the location, together with elevation, ellipticity (Dziewonski and Gilbert, 1976; Kennett and Gudmundsson, 1996; Engdahl et al., 1998), and depth-phase bounce point corrections (Engdahl et al., 1998). The application of two single-event location algorithms currently in use for global earthquake location provides the necessary quality assurance to produce highly accurate event locations for the ISC-GEM catalogue.

For the early instrumental period (1904-1963) where the ISC-GEM data collection effort provided data from the scanned ISS bulletins (Villaseñor and Engdahl, 2005; 2007), original station reports from the ISC archives and the Gutenberg notepads, we obtain the initial estimates of event hypocentres using the new ISC location algorithm. For the modern instrumental period (1964-2009) where no substantial volume of station readings has been added to the ISC database, we simply use the preferred solution from the ISC bulletin.

Using the initial ISC locations described above, the locations and depths of all events included in the ISC-GEM catalogue are first determined using the EHB algorithm. In the absence of depth constraint by local station phase data, the EHB algorithm provides a comprehensive analysis of reported phases that can significantly improve event depth estimates by identifying and utilizing near-event surface reflections (depth phases). The new ISC location algorithm is used next with earthquake depths fixed to those from the EHB analysis. The ISC algorithm provides independent depth confirmation using depth phase stacking and also provides more accurate hypocentre locations by taking correlated travel-time prediction error structure into account.

#### Earthquake depth determination

Depth phases provide important constraints on event depth because their travel time derivatives with respect to depth are opposite in sign to those of the direct P phase. Depth to origin time trade-off is also avoided by the inclusion of depth phases. These phases are commonly reported as pP or sP (a P-wave or S-wave reflecting off of a hard rock interface, respectively) or as pwP (a P-wave reflected off the ocean or ice surface). However, as often as not these phases are simply reported as unidentified phase arrival times. With knowledge of an event depth and distance, potential depth phase arrivals are re-identified following each iteration in the EHB procedure using a

probabilistic association algorithm. Probability density functions (PDF) for depth phases and the PcP phase, centered on their theoretical relative travel times for a given hypocenter, are compared to the observed phase arrivals. When PDFs overlap for a particular depth phase, phase identification is assigned in a probabilistic manner based on the relevant PDF values, making sure not to assign the same phase to two different arrivals. This procedure works relatively well in an automatic fashion, but the phase identifications can depend heavily on the starting depth, which in most cases is not well known. Hence, depth phase identifications for every event in the ISC-GEM catalogue have been manually scrutinized for the possibility of an erroneous local minimum in depth because of a poor starting depth and adjusted accordingly. Normally, at least five corroborating depth phases are necessary for an EHB depth to be accepted.

In order to determine pwP arrival times and correct all depth phases for topography or bathymetry at their reflection points on the earth's surface, it is necessary to first determine the latitude and longitude of these bounce points and then the corresponding seafloor depth or continental elevation. Bounce point coordinates are easily computed from the distance, azimuth and ray parameter of the depth phase (pP in the case of pwP). The NOAA ETOPO1 global relief file (Amante and Eakins, 2009) was averaged over 5 x 5 minute equal area cells and then projected on a 5 x 5 minute equi-angular cell model using a Gaussian spatial filter. The use of a smoothed version of ETOPO1 is justified because the reflection of a depth phase does not take place at one single point, but over a reflection zone with a size determined by the Fresnel zone of the wave. The maximum half width of a ray with a wavelength of 10 km and a ray path length of 1000 km is estimated to be 36 km (Nolet, 1987). The topographic and bathymetric information in this version of ETOPO1, with elevations

referred to land or sea bottom, is used to determine the correction for bounce point elevation/depth, which is added to the computed travel times for depth phases. Theoretical times are not computed for pwP phases in the case of bounce point water depths  $\leq 1.5$  km because it is nearly impossible to separate the pP and pwP arrivals on most records (about 2s separation).

Despite the general success of the EHB procedures for depth determination, there remain some issues that must be taken into account. For example, the relative frequency (or amplitude) of depth phase observations is sensitive to local structure at bounce points. Many depth phases reflect in the vicinity of plate boundaries where the slopes of surface reflectors are large (> 1 degree). Reflections at a dipping reflection zone may lead to small asymmetries in depth phase waveforms and, may influence their relative amplitudes, resulting in a greater potential for phase mis-identifications. In addition, for short-period (1s) waves, water-sediment interfaces at the sea bottom may have small impedance contrasts. Consequently, on short-period seismograms the amplitude of a pwP phase may be comparable to or larger than the pP phase reflecting at the sea bottom, and pwP may easily be mis-identified as pP.

One outstanding issue is that for large shallow-focus complex earthquakes pP often arrives in the source-time function of the P phase, which may consist of one or more sub-events. The gross features of the source-time functions of P and pP, however, remain discernible in broadband displacement records and the exact onset times of depth phases can be further refined by examination of velocity seismograms that are sensitive to small changes in displacement. For the GEM project we have relied primarily on reported phase arrival times, usually read from short-period seismograms. However, for large complex events EHB depths ordinarily have to be

set to depths published by USGS/NEIC that have been determined by rigorous analysis of phase arrival times read from broadband seismograms.

Finally, there are many events in the ISC-GEM catalogue for which there are no reported depth phases or for which those that were reported are inconsistent, especially in the earlier part of the 20<sup>th</sup> century. For these events a nominal depth is adopted, based on the depth distribution of neighboring events that are well constrained in depth and are consistent with other event depths in that tectonic setting. For every subduction zone worldwide, all ISC-GEM events were plotted in cross section with respect to the arc center of curvature to assist in setting depths of those events that have no other available depth constraints.

#### Earthquake epicentre and origin time determination

In the next step of ISC-GEM location procedures we determine the earthquake epicenter and origin time parameters by fixing the depth to that obtained from the EHB analysis. The EHB location and origin time are used as the initial guess for the ISC locator. The ISC location algorithm can further refine the locations because it reduces the location bias introduced by the correlated travel-time prediction error structure due to unmodeled 3D heterogeneities in the Earth.

Figure 1 shows the total number of associated phases and those that are used in the location in each year. As the number of phases increases almost exponentially in time, the number of phases traveling along similar ray paths increases accordingly, contributing more and more to the potential location bias. Thus, accounting for the correlated error structure becomes imperative.

Figure 2 compares deviations between the EHB and corresponding ISC locations for events in the ISC-GEM catalogue. The median location difference is 9 km, that is,

50% of the locations are within 9km of each other. Furthermore, 90% of the location differences are less than 20 km. Given that the ISC-GEM catalogue locations are predominantly teleseismic, the EHB and ISC locations show remarkable consistency. Figure 2b shows the location deviations with respect to the EHB locations. The plot indicates that there is no bias between the EHB and ISC locations.

Even though the depth is fixed to the EHB depth, the ISC location algorithm may obtain an independent depth estimate through the depth-phase stacking (Murphy and Barker, 2006) provided that sufficient number of first-arriving P and depth-phase pairs are available. Some 65% of the events in the ISC-GEM catalogue also have depth estimates from the depth phase stacking. Figure 3 shows an excellent agreement between the depths obtained through the EHB depth determination procedures and the depth-phase stacking.

#### **Uncertainty estimates**

Accounting for correlated errors not only reduces location bias, but also provides more accurate uncertainty estimates. Most location algorithms assume independent, normally distributed observational errors. Unfortunately, this assumption rarely holds because the 1D global average velocity model used in the location does not capture all the 3D velocity heterogeneities and travel-time predictions along similar ray paths become correlated, decreasing the effective number of degrees of freedom. Because the number of independent observations is less than the total number of observations used in the location, the assumption of independence inevitably leads to underestimated uncertainty estimates. Since the ISC location algorithm uses the effective number of degrees of freedom, the formal location uncertainties described by the *a posteriori* model covariance matrix become larger, resulting in enlarged and more circular error ellipses. Figure 4 shows the distribution of origin time uncertainty

and the area of the error ellipse, both scaled to the 90% confidence level. The median origin time uncertainty is 0.25s and the median area of the error ellipse is  $105 \text{ km}^2$ .

Because the depth is fixed to the EHB depth, no formal depth uncertainties can be calculated by the ISC locator. In order to provide a depth uncertainty, we use the depth-phase depth uncertainty from the depth phase stacking, if available. These are typically the events where the EHB depth determination procedures relied on the reported depth phases. If no depth-phase stack exists for an event we estimate the depth uncertainty as the median absolute deviation of the depths in the corresponding ISC default depth grid cell if it exists, otherwise we set the depth uncertainty to a nominal 25 km. Note that the ISC default depth grid cells are only defined if there are sufficient number of observations with a limited 25 to 75 percentile range (see Bondár and Storchak, 2011); therefore the median absolute deviation of the depths in a grid cell is typically smaller than 15 km.

Besides the formal location uncertainty estimates, measures of the network geometry may also indicate the quality of the location. Figure 5 shows the cross-plot of secondary azimuthal gap and the eccentricity of the error ellipse for all candidate events processed for the ISC-GEM catalogue. The secondary azimuthal gap is defined as the largest azimuthal gap filled by a single station (Bondár et al., 2004). The eccentricity varies between 0 and 1; at zero eccentricity the error ellipse becomes a circle, indicating evenly distributed stations around the event, while the error ellipse degenerates to a line at a unit eccentricity, indicating that all stations aligned at a single azimuth from the event.

We consider events having the most accurate locations as those that are recorded with a secondary azimuthal less than  $120^{\circ}$  and with an error ellipse eccentricity less than

0.75, or those that qualify for GT5 candidate (Bondár and McLaughlin, 2009b). Out of the 19,711 earthquakes that we have processed 14,517 locations belong to this category; 12,570 events also have independent depth estimates from the depth-phase stacking.

Events recorded with a huge secondary azimuthal gap (sgap  $\geq 270^{\circ}$ ) or events recorded only with a small number of stations (nsta  $\leq 5$ ) are considered unreliable locations and are listed in the Supplementary of the main ISC-GEM catalogue. Note that there are only 45 events relegated to the Supplementary catalogue based on the location accuracy measures; the vast majority of the 903 events listed in the Supplementary catalogue are there because they had an insufficient number of amplitude-period observations to calculate  $M_S$  or  $m_b$ . About half of the events in the Supplementary catalogue have the most accurate location and depth estimates, and many of them are deep events. Thus, for studies that do not require magnitude estimates, it is safe to use the locations listed in the Supplementary catalogue.

#### Earthquake relocation results

The ISC-GEM catalogue consists of 18,808 earthquakes between 1900 and 2009. Apart from 10 events between 1900 and 1903, for which we adopt the hypocentre parameters from the Abe catalogue (Abe, 1981, 1984; Abe and Noguchi, 1983a, 1983b), we relocated all earthquakes using the two-step location procedure described above.

One of the major objectives of this project was to provide improved hypocentre estimates for events in the ISC-GEM catalogue. To achieve this goal we launched an ambitious data entry effort to add station readings that did not previously exist in

digital form. For events occurring between 1904 and 1963 some 1,200,000 observations were entered into the database either from the station reports in the ISC archive or by digitizing the scanned images of the ISS bulletin (Villaseñor and Engdahl, 2005; 2007). Of the total number of added phases some 600,000 are P-type phases, 300,000 are S-type phases, and the rest are amplitude readings. Some 665,000 P and S type phases contributed to the relocation of events in the historical period. Although no substantial amount of new phase data were acquired for the modern period (1964-2009), the number of phases used in the location has still dramatically increased. Recall that in the past the vast majority of locations in the ISC bulletin were obtained using only first-arriving Pg, Pn and P phases. The number of defining phases used in the location in the modern period increased from 5,373,783 to 8,323,546 owing to fact that both the EHB and ISC locators use most *ak135* phases in the location.

Figure 6 shows the box-and-whisker plots of the median number of stations and the median secondary azimuthal gap (largest azimuthal gap filled by a single station) in each decade. The box in a box-and-whisker plot shows the range between first (25%) and third (75%) quartiles, and the band inside the box represents the second (the median) quartile. The ends of the whiskers indicate the minimum and maximum of the data. As the number of stations used in the location increases with time, the median secondary azimuthal gap decreases and levels off around 45°.

The preferred locations before the ISC-GEM project constituted a mixture of locations from the Abe (Abe, 1981, 1984; Abe and Noguchi, 1983), the Centennial (Engdahl and Villaseñor, 2002), the ISS (Villaseñor and Engdahl, 2005; 2007) and the ISC catalogues. We compare these locations (before) to the ISC-GEM locations (after). Figure 7 shows the locations before and after the ISC-GEM relocations for the

entire period, 1900-2009. Even at the global scale it is apparent that the earthquake locations are better clustered in the ISC-GEM catalogue. In the historical period many event depths were fixed to the surface; due to the better depth estimates, this artifact is removed from the ISC-GEM catalogue.

Figure 8 shows the distributions of location and depth differences before and after the ISC-GEM relocations. The median distance between the before and after locations is 10km. 90% of the events moved by less than 25km, and 90% of the depth changes are between  $\pm 20$ km.

We expect that the largest differences between the before and after ISC-GEM relocations will come from the early years. Figures 9-10 show the box-and-whisker plots of the location, depth and origin time differences in each decade. Indeed, most of the large location changes occur in the first half of the century; the effect of improved depth estimates can be seen through the entire period but large variations level off with time.

Recall that for about one-third of the events had no depth phase information, and therefore their depth were fixed to a depth that is consistent with the depth of other events in that particular tectonic setting. Although this carries a small risk that the depth of intraplate events might have been adjusted to an interplate boundary, we have by no means forced event hypocenters to occur on plate boundaries, but we had rather let the data decide the best location estimate. An erroneous depth for an intraplate (as a matter of fact, for any) event would generate large residuals and prompted us to carry out a more involved study to get the hypocenter right. Since hypocentres in the first part of the 20<sup>th</sup> century were the most vulnerable to large location errors, we manually reviewed every single event occurring between 1903 and

1930 in the ISC-GEM catalogue as well as all other problematic events. Furthermore, the quality of the event locations and depths are not only described with their formal uncertainties but with qualitative flags ranging from A to D. Events with depth fixed to the corresponding tectonic setting, or epicentres determined by a poor network geometry are never considered the best quality and given the lowest level quality flags.

#### Conclusions

The ISC-GEM Global Instrumental Catalogue represents the final product for one of the global components of the GEM project. The ISC-GEM catalogue consists of 18,809 large and moderate earthquakes that have occurred during the 110-year period between 1900 and 2009. The ISC-GEM bulletin contains some 13 million phases associated with the earthquakes in the catalogue.

One of the requirements from the GEM project was that each event in the ISC-GEM instrumental catalogue is characterized by a measure of magnitude. For a number of events without a direct measure of  $M_W$  there were insufficient number of amplitude measurements to calculate either  $m_b$  or  $M_s$ , Furthermore, since body wave magnitudes were regularly reported only from the second half of the 20<sup>th</sup> century, many deep events from the early period has no magnitude estimate and therefore cannot be included in the main ISC-GEM catalogue. We felt the need to create a Supplementary catalogue to the ISC-GEM catalogue that contains the 858 large earthquakes with no magnitude estimates, as well as 45 events with less reliable locations. Hence, for seismicity studies that do not require magnitude information, events in the Supplementary catalogue can be joined with the main ISC-GEM catalogue.

All events (except for 10 events between 1900 and 1903) in the ISC-GEM catalogue are relocated using uniform and rigorous location procedures. During the project an unprecedented amount of phase arrival data were scanned, digitized and archived in the ISC database. Owing to the ISC-GEM location procedures and to the substantial increase in the volume of observational data used in the relocations, the ISC-GEM catalogue offers an improved view of the seismicity of the Earth. The ISC-GEM locations are better clustered and considerably reduce scatter in location estimates. The significantly improved depth estimates provide a better resolution of earthquakes associated with subducting slabs.

The ISC-GEM Global Instrumental Earthquake Catalogue (1900-2009) is made publicly available at the ISC website, <u>www.isc.ac.uk</u>. The ISC-GEM catalogue is regularly updated based on the feedback from researchers. The changes are documented at <u>www.isc.ac.uk/iscgem/update\_log</u>.

#### Acknowledgements

This project was sponsored by the GEM Foundation. We are grateful to Nobuo Hamada (Japan Meteorological Agency, emeritus, Japan) who provided a digital copy of JMA historical bulletin data for 1923-1970 and Katsuyuki Abe for making available a CD-ROM with the catalogue of Abe and Noguchi. We wish to recognize the initiative of the late Edouard Arnold and Pat Willmore, former Directors of the ISC, for transferring a large fraction of the ISS paper bulletins onto punched cards and preparing the Shannon tape. We also wish to acknowledge the effort of Tom Boyd, Colorado School of Mines, USA, for his contribution in correcting the data on the

Shannon tape. We also thank George Helffrich, Emile Okal and an anonymous reviewer for their thorough review of the manuscript.

#### References

Abe, K., 1981. Magnitudes of large shallow earthquakes from 1904 to 1980, *Phys. Earth Planet. Int.*, **27**, 72-92.

Abe, K., and S. Noguchi, 1983a. Determination of magnitudes for large shallow earthquakes, 1898-1917, *Phys. Earth Planet. Inter.*, **32**, 45-59.

Abe, K., and S. Noguchi, 1983b, Revision of magnitudes of large shallow earthquakes 1897 – 1912, *Phys. Earth Planet. Int.*, **33**, 1-11.

Abe, K., 1984. Complements to "Magnitudes of large shallow earthquakes from 1904 to 1983", *Phys. Earth Planet. Int.*, **34**, 17-23.

Amante, C., and B.W. Eakins, 2009. ETOPO1 1 arc-minute global relief model: Procedures, data sources and analysis, *NOAA Technical Memorandum NESDIS NGDC-24*.

Båth, M., and S.J. Duda, 1979. Some aspects of global seismicity. *Tectonophysics*, **54**, TI-T8.

Bondár, I., S.C. Myers, E.R. Engdahl, and E.A. Bergman, 2004. Epicenter accuracy based on seismic network criteria, *Geophys. J. Int.*, **156**, 483-496, doi: 10.1111/j.1365-246X.2004.02070.x.

Bondár, I., and K. McLaughlin, 2009a. Seismic location bias and uncertainty in the presence of correlated and non-Gaussian travel-time errors, *Bull. Seism. Soc. Am.*, **99**, 172-193.

Bondár, I., and K. McLaughlin, 2009b. A new ground truth data set for seismic studies, *Seism. Res. Let.*, **80**, 465-472.

Bondár, I., and D. Storchak, Improved location procedures at the International Seismological Centre, 2011. *Geophys. J. Int.*, **186**, 1220-1244, doi:10.1111/j.1365-246X.2011.05107.x.

Di Giacomo, D., J. Harris, A. Villaseñor, D.A. Storchak, E.R. Engdahl, W.H.K. Lee, and the Data Entry Team, 2013. ISC-GEM: Global Instrumental Earthquake Catalogue (1900-2009), I. Data collection from early instrumental seismological bulletins, *Phys. Earth Planet. Int.*, submitted.

Di Giacomo, D., I. Bondár, D.A. Storchak, E.R. Engdahl, P. Bormann, and J. Harris, 2013. ISC-GEM: Global Instrumental Earthquake Catalogue (1900-2009), III. Re-computed  $M_S$  and  $m_b$ , proxy  $M_W$ , final magnitude composition and completeness assessment, *Phys. Earth Planet. Inter.*, submitted.

Dziewonski, A.M., and F. Gilbert, 1976. The effect of small, aspherical perturbations on travel times and a re-examination of the correction for ellipticity, *Geophys. J. R. Astr. Soc.*, **44**, 7-17.

Engdahl, E.R., R. van der Hilst, and R. Buland, 1998. Global teleseismic earthquake relocation with improved travel times and procedures for depth determination, *Bull. Seism. Soc. Am.*, **88**, 722-743.

Engdahl, E.R., and A. Villaseñor, Global Seismicity: 1900–1999, 2002. in W.H.K.

Lee, H. Kanamori, P.C. Jennings, and C. Kisslinger (editors), *International Handbook* of Earthquake and Engineering Seismology, Part A, Chapter 41, 665–690, Academic Press.

Gutenberg, B., and C. F. Richter, 1954. Seismicity of the Earth and Associated Phenomena. *Princeton Univ. Press*, Princeton, N.J., 310 pp.

Kennett, B.L.N., E.R. Engdahl, and R. Buland, 1995. Constraints on seismic velocities in the Earth from traveltimes, *Geophys. J. Int.*, **122**, 108-124.

Kennett, B.L.N., and O. Gudmundsson, 1996. Ellipticity corrections for seismic phases, *Geophys. J. Int.*, **127**, 40-48.

Murphy, J.R., and B.W. Barker, 2006. Improved focal-depth determination through automated identification of the seismic depth phases pP and sP, *Bull. Seism. Soc. Am.*, **96**, 1213-1229.

Nolet, G., 1987. Seismic wave propagation and seismic tomography, in *Seismic Tomography*, pp. 1-23, ed. Nolet, G., Reidel, Dordrecht.

Pacheco, J. F., and L. R. Sykes, 1992. Seismic moment catalog of large shallow earthquakes, 1900 to 1989. *Bull. Seism. Soc. Am.* **82**, 1306-1349.

Storchak, D.A., J. Schweitzer, and P. Bormann, 2003. The IASPEI Standard Seismic Phase List, *Seismol. Res. Lett.* 74, 6, 761-772.

Storchak, D.A., J. Schweitzer, and P. Bormann, 2011. Seismic phase names: IASPEI Standard, in *Encyclopedia of Solid Earth Geophysics*, 1162-1173, Ed. H.K. Gupta, Springer.

Storchak, D.A., D. Di Giacomo, E.R. Engdahl, I Bondár, W.H.K. Lee and P.
Bormann, 2013. The ISC-GEM global instrumental earthquake catalogue (1900-2009): Introduction, *Phys. Earth Planet. Inter.*, submitted.

Utsu, T., 1979. Seismicity of Japan from 1885 through 1925, A new catalog of earthquakes of M > 6 felt in Japan and smaller earthquakes which caused damage in Japan (in Japanese with English abstract). *Bull. Earthquake Res. Inst.* **54**, 253-308.

Utsu, T., 1982a. Seismicity of Japan from 1885 through 1925 (Correction and supplement) (in Japanese with English abstract). *Bull. Earthquake Res. Inst.* **57**, 111-117.

Utsu, T., 1982b. Catalog of Large earthquakes in the region of Japan from 1885 through 1980 (in Japanese with English abstract). *Bull. Earthquake. Res. Inst.*, **57**, 401-463.

Villaseñor, A., and E.R. Engdahl, 2005. A digital hypocenter catalog for the International Seismological Summary, *Seism. Res. Let.*, **76**, 554-559.

Villaseñor, A., and E.R. Engdahl, 2007. Systematic relocation of early instrumental seismicity: Earthquakes in the International Seismological Summary for 1960-1963, *Bull. Seism. Soc. Am.*, **97**, 1820-1832.

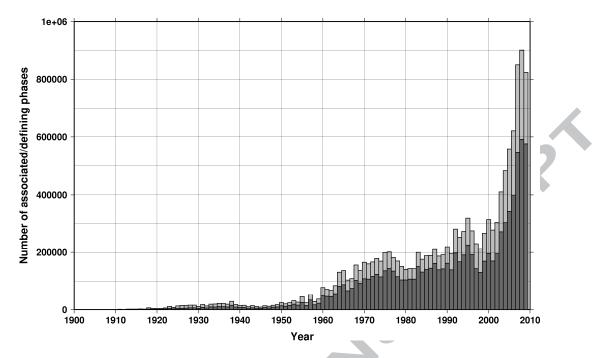


Figure 1. Annual number of associated (gray) and defining (dark gray) phases in the ISC-GEM catalogue. A defining phase is a phase that was used in the location.

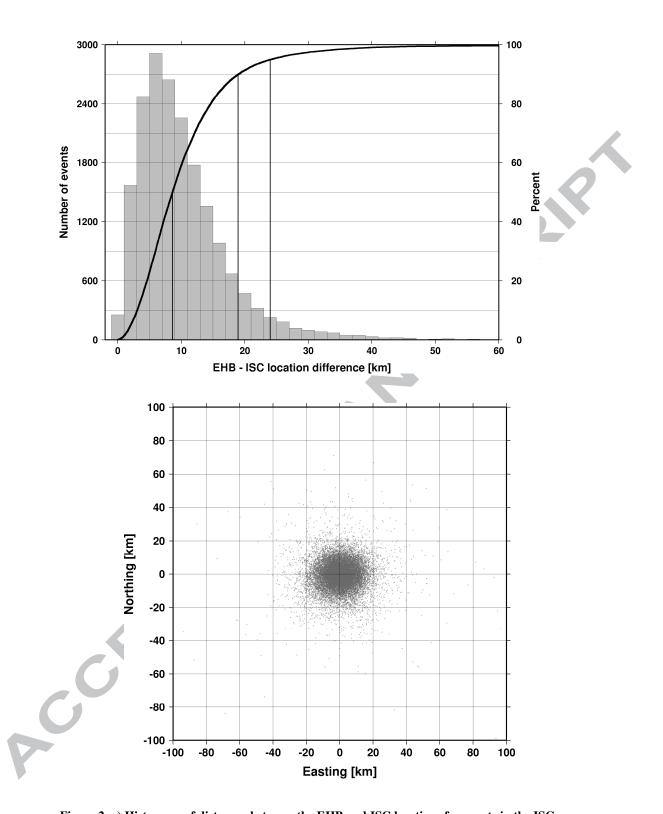


Figure 2. a) Histogram of distances between the EHB and ISC locations for events in the ISC-GEM catalogue. The 50% (median), 90% and 95% percentile points on the cumulative distribution (thick line) are marked the vertical lines.. b) The deviations between the EHB and ISC locations show no bias.

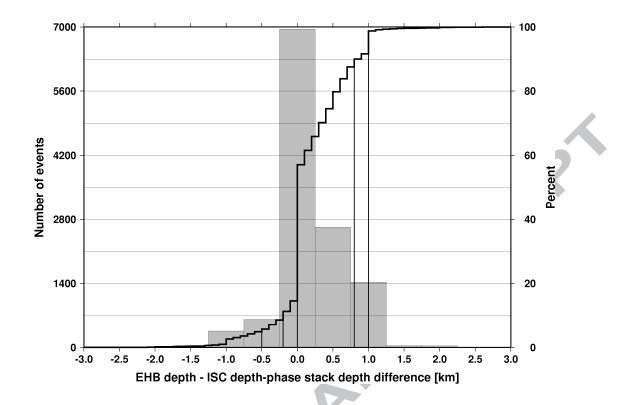


Figure 3. Histogram of the difference between the depth estimates from depth phase stacking and the EHB depth determination. The 5%, 10%, 50%, 90% and 95% percentile points on the cumulative distribution (thick line) are indicated by the vertical lines.

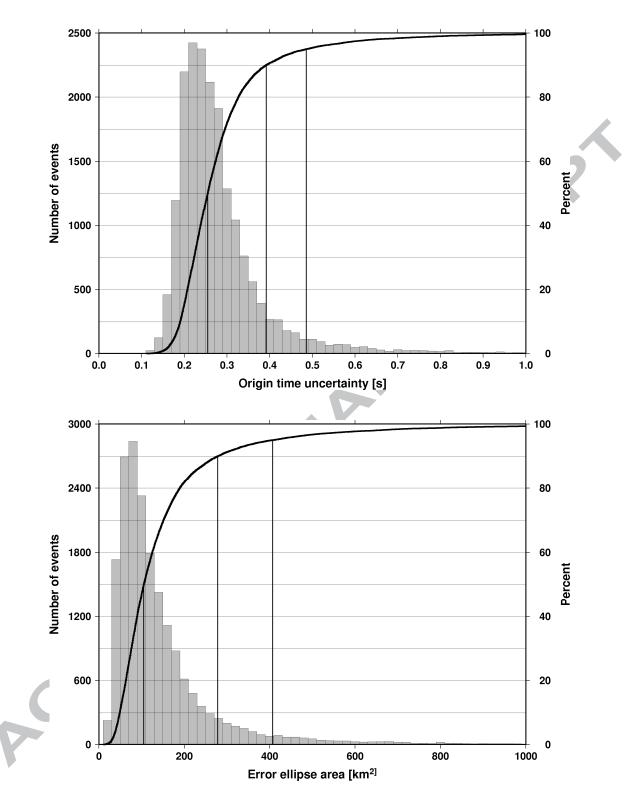


Figure 4. Histograms of the a) origin time uncertainty, and b) area of the 90% confidence error ellipse for events in the ISC-GEM catalogue. The 50% (median), 90% and 95% percentile points on the cumulative distribution (thick line) are marked by the vertical lines.

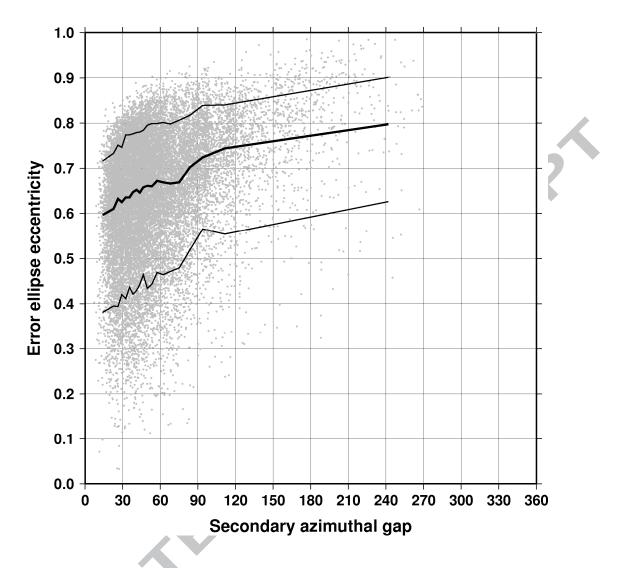


Figure 5. Error ellipse eccentricity as a function of secondary azimuthal gap. The thick line indicates the median curve; the 10% and 90% percentile curves are drawn by thin lines.

RCC

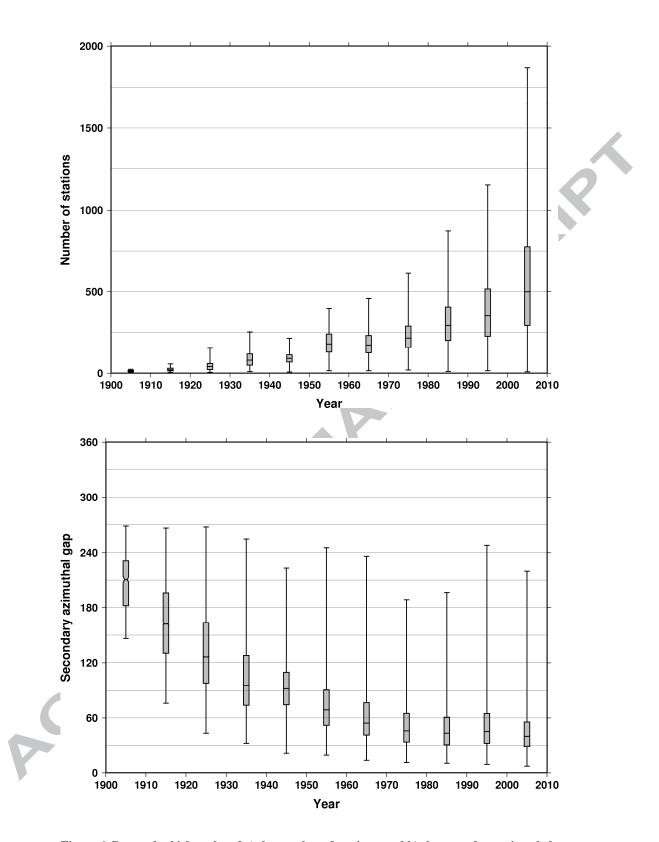
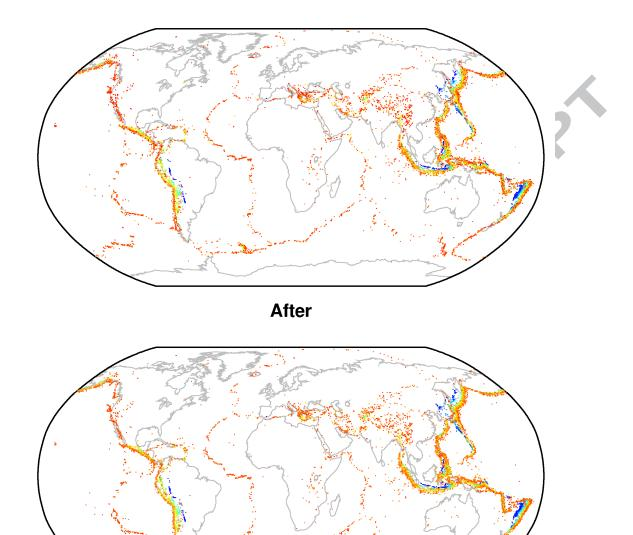


Figure 6. Box-and-whisker plot of a) the number of stations, and b) the secondary azimuthal gap in each decade. The gray boxes represent the 25% - 75% quartile ranges; the vertical extent of the lines indicate the full, minimum to maximum range.

Before



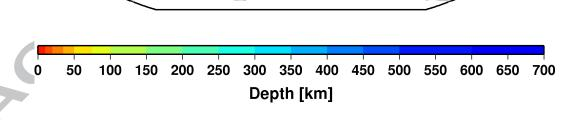


Figure 7. Preferred locations before and after the ISC-GEM relocations. The ISC-GEM locations show an improved view of the seismicity of the Earth.

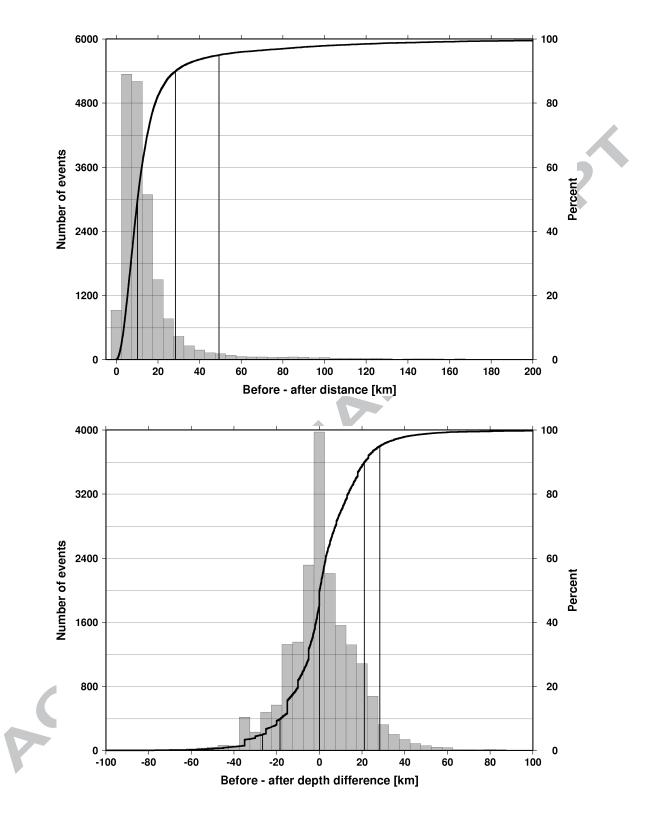


Figure 8. Distribution of a) location, and b) depth differences before and after the ISC-GEM relocations. The 50% (median), 90% and 95% percentile points on the cumulative distributions (thick line) are marked with the vertical lines.

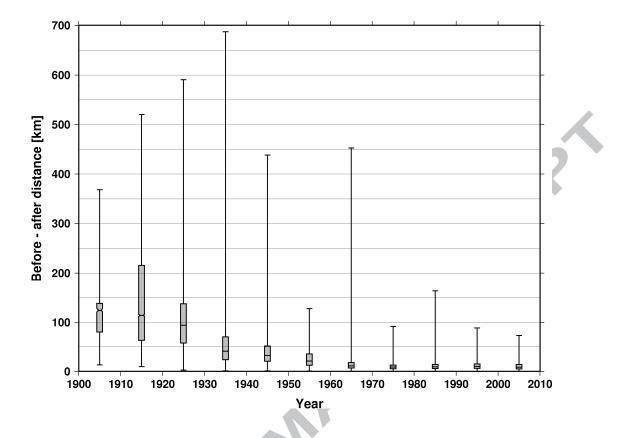


Figure 9. Box-and-whisker plot of the location differences before and after the ISC-GEM relocations in each decade. The gray boxes represent the 25% - 75% quartile ranges; the vertical extent of the lines indicate the full, minimum to maximum range. Event locations change the largest extent in the first three decades.

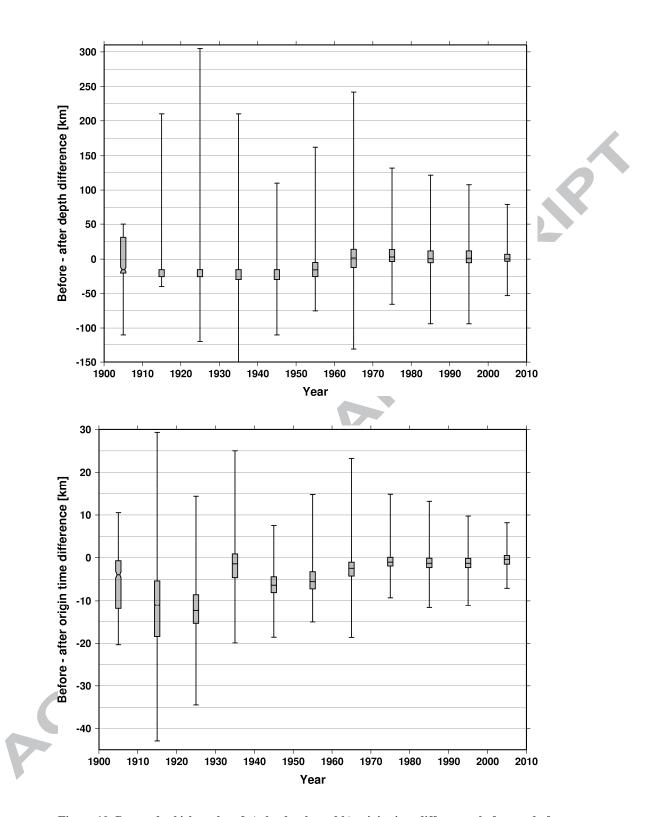


Figure 10. Box-and-whisker plot of a) the depth, and b) origin time differences before and after the ISC-GEM relocations in each decade. The gray boxes represent the 25% - 75% quartile ranges; the vertical extent of the lines indicate the full, minimum to maximum range. The

apparent bias in the first six decades is due to the fact that previously many event depths were Acceleration

fixed to the surface.

#### Highlights

- We present the ISC-GEM Global Instrumental Earthquake Catalogue ٠
- We cover 100+ year of seismicity

- We relocated all events based on instrumental data
- ٠ We made the ISC-GEM catalogue available at the ISC website